

Article

# Design and Implementation of a Dual-Axis Tilting Quadcopter

Ali Bin Junaid <sup>1</sup>, Alejandro Diaz De Cerio Sanchez <sup>2</sup>, Javier Betancor Bosch <sup>2</sup>, Nikolaos Vitzilaios <sup>3</sup> and Yahya Zweiri <sup>2,4,\*</sup> 

<sup>1</sup> Department of Mechanical Engineering, KU Leuven, 3000 Leuven, Belgium; ali.binjunaid@kuleuven.be

<sup>2</sup> Faculty of Science, Engineering and Computing, Kingston University London, London SW15 3DW, UK; aldiazde@gmail.com (A.D.D.C.S.); J.Betancorbosch@kingston.ac.uk (J.B.B.)

<sup>3</sup> Department of Mechanical Engineering, University of South Carolina, Columbia, SC 29208, USA; VITZILAIOS@sc.edu

<sup>4</sup> Khalifa University Center for Autonomous Robotic Systems, Department of Aerospace Engineering, Khalifa University of Science and Technology, P.O. Box 127788 Abu Dhabi, UAE

\* Correspondence: Y.Zweiri@Kingston.ac.uk; Tel.: +44-020-8417-4846

Received: 7 August 2018; Accepted: 18 October 2018; Published: 20 October 2018



**Abstract:** Standard quadcopters are popular largely because of their mechanical simplicity relative to other hovering aircraft, low cost and minimum operator involvement. However, this simplicity imposes fundamental limits on the types of maneuvers possible due to its under-actuation. The dexterity and fault tolerance required for flying in limited spaces like forests and industrial infrastructures dictate the use of a bespoke dual-tilting quadcopter that can launch vertically, performs autonomous flight between adjacent obstacles and is even capable of flying in the event of the failure of one or two motors. This paper proposes an actuation concept to enhance the performance characteristics of the conventional under-actuated quadcopter. The practical formation of this concept is followed by the design, modeling, simulation and prototyping of a dual-axis tilting quadcopter. Outdoor flight tests using tilting rotors, to follow a trajectory containing adjacent obstacles, were conducted in order to compare the flight of conventional quadcopter with the proposed over-actuated vehicle. The results show that the quadcopter with tilting rotors provides more agility and mobility to the vehicle especially in narrow indoor and outdoor infrastructures.

**Keywords:** aerial robotics; quadcopters; UAVs; dual-tilting; tilting rotors; over-actuation; flight control; rotorcraft

## 1. Introduction

Over the last few decades, the usage and deployment of UAVs (Unmanned Aerial Vehicles) have been growing, from hobby to military applications. Some of those applications include surveying, maintenance and surveillance tasks, transportation and manipulation, search and rescue [1,2]. Rotorcraft UAVs are of particular interest as they offer advanced capabilities such as Vertical Take Off and Landing (VTOL) and high agility. Quadcopters are the most researched and used platforms in this area.

A quadcopter's lift and thrust is generated by four propellers mounted on high-speed, high-power brushless DC motors. Quadcopters use an electronic control system and electronic sensors to stabilize themselves. With their small size and VTOL capability, quadcopters can fly indoors as well as outdoors. Similar to a conventional helicopters, quadcopters can hover but have significant other advantages such as ease of piloting and mechanical simplicity. Recently, there is a rapid growth in quadcopter development due to the high potential used in numerous commercial applications.

For real world applications, quadcopters require more payload capacity and should be more invulnerable and robust towards external disturbances. However, increased payload capacity demands up scaling the platforms which eventually results in decreased maneuverability and agility [3]. As stated in [3], the inertia of the platform is increased and requires larger control moments to achieve higher agility with the increase of the vehicle size. Secondly, the increased weight results in increased propeller size consequently increasing the inertia. The conventional quadcopter possesses such physical constraints with its control on larger scales.

Conventional quadcopters are under-actuated mechanical systems possessing less control inputs than Degrees Of Freedom (DOFs). Over the last decades, different control techniques have been proposed to deal with the quadcopter under-actuation for an effective and more controlled performance [3–5]. Still, the under-actuation of quadcopter has limitations on its flying ability in free or cluttered space.

In a conventional under-actuated quadcopter, actuators failure results in complete destabilization of the vehicle as its control is completely dependent on the symmetry of the lift. To alleviate this problem, several approaches have been proposed in previous studies. In [6], propellers with variable pitch and shifting of the Center of Gravity (COG) are suggested. These approaches enable to achieve the controllability of the vehicle in roll and pitch axes up to some extent. However, the yaw axis still remains uncontrollable. In [7], a bounded control law was proposed in order to have a safe landing for quadcopter in case of actuators failure.

One approach to overcome this issue is to increase the number of rotors. Typical example includes 4Y octocopters [8]. This approach has advantages such as the mechanical simplicity and reliability. However, this approach results in increased weight and increased inertia hence reducing the agility of the vehicle. Furthermore, increased number of rotors results in larger power consumption which immensely impacts the endurance of the aircraft. Nevertheless, standard hexarotors are not fail-safe multi-rotor platforms and cannot hover with five propellers [9].

Apart from the increasing number of rotors approach, other approaches include variation in the types of actuators keeping in consideration the key factors which are the vehicle's size and weight. Cutler et al. [10] showed an effective approach by using propellers with variable pitch. In this approach, while keeping the weight down, the bandwidth of its actuators was increased. However, actuator failure resulting in instability still remains an issue.

Other solutions to overcome the under-actuated problem include tilt-wing mechanisms [11], UAVs with non-parallel fixed thrust directions [12], or tilt-rotor actuations [13]. Similar approach with the dual-axis tilting of the rotors providing the broad range of control bandwidth for the same number of rotors is proposed in [14]. However, most of the platforms were developed and tested in indoor environments with low payload capacities. Furthermore, indoor navigation systems were used to develop the control of the tilting quadcopter. Similar concept of rotor tilting is used in [15,16], however, rotor tilting is limited to single axis only.

In [17], Control Moment Gyroscopes (CMG) were proposed to increase the control system bandwidth by merging a thrust vectoring approach with additional flywheels in order to be used as CMG, and a vane system for thrust vectoring. However, the extra weight of the flywheels and the thrust vectoring vane system results in increased weight of the aircraft and complicates the design of the vehicle. Gress [18] used Opposed Lateral Tilting (OLT) technique for using the gyroscopic effects for governing the pitch attitude of aircraft, using the propellers as gyroscopes. In [19], OLT proved to achieve higher controllability. The detailed model and control strategy for hovering, with experimental evidence is presented in [20]. To implement such control strategies and actuation mechanisms, it is important to keep in mind key factors for the development of such vehicles, which are weight, mechanical simplicity, cost-effectiveness and ability to manufacture the platform in less time.

Nowadays, advances in the fields of Computer Aided Design (CAD) and Rapid Prototyping (RP) have provided the tools to rapidly generate a prototype from a concept. RP technique allows to automatically construct physical models using additive manufacturing technology [21,22]. Mechanical parts or assembly can be quickly manufactured using 3D CAD design. This technique has

emerged as an innovative tool to reduce the time and cost of manufacturing and fabrication by creating 3D product directly from computer aided design providing the ability to perform design validation and analysis [23,24].

This paper presents design and implementation of a novel actuation strategy which was proposed by co-author in [25] in order to increase the agility and control bandwidth of the conventional quadcopters in outdoor scenarios.

The introduction of dual-axis tilting to the propellers produces an over-actuated quadcopter with ability to have 12 control inputs with 6 control outputs. The tilting of propellers provides the necessary gyroscopic effects to provide fast control and action. The proposed tilting rotor solution for quadcopter uses additional 8 servomotors that allow the rotors to tilt in both axes, an over-actuated system can potentially track an arbitrary trajectory over time. As shown in [26,27], with single axis tilting, full controllability over the quad-rotor position and orientation provides possibility of hovering in a tilted configuration. The research here focuses on the design of such platform and conduct initial experiments to test the actuation modules in outdoor urban environment.

The development of the proposed concept is mainly based on arm design of the quadcopter in which each arm is able to generate three-actuation independently, including the rotors to achieve differential thrusting and dual tilting mechanism to provide broad range of control bandwidth. The computer-aided design (CAD) model was designed and analyzed using finite element analysis (FEA) for the structural rigidity and stability. The experiments were performed using the developed platform which achieved full controllability of the quadcopter thus transforming the system into an over-actuated machine. Flight tests were performed in a trajectory having sharp corners between adjacent obstacles in order to compare the behavior of conventional quadcopter configuration and the proposed actuation strategy. The results show that the quadcopter with tilting rotors provides more agility and mobility to the vehicle especially in narrow indoor and outdoor infrastructures.

The paper layout is as follows: first the design approach for the development of quadcopter with over-actuated mechanism along with its electronics to control the mechanisms is presented. Secondly, the modeling and simulation results are presented. Furthermore, the structural analysis of the rapid prototyped parts is presented ensuring the structural stability of the platform. The flight test results of the developed platform for the conventional and over-actuated configuration are presented. Finally, the results are discussed and some conclusions are drawn.

## 2. Design Approach

Two servomotors were used to achieve the dual tilting actuation with each rotor. The platform was designed in SolidWorks<sup>®</sup> and manufactured using a ZORTRAX 3D printer [28]. The mechanical design of the quadcopter is shown in Figure 1.

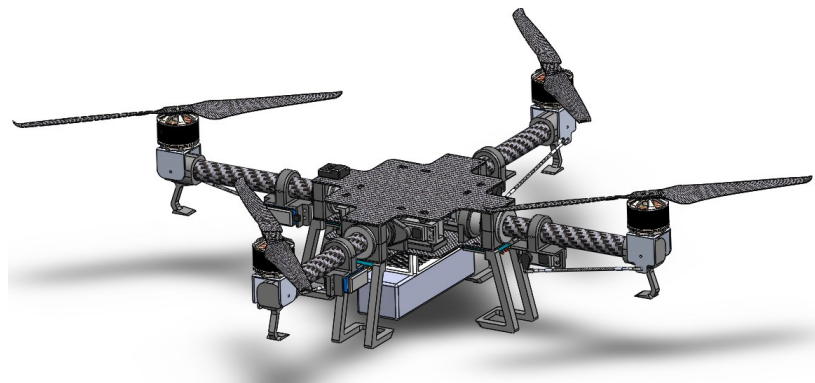


**Figure 1.** CAD model of proposed quadcopter.

The proposed actuation concept of the quadcopter arms and motors is shown in Figures 2 and 3. The dual tilting mechanism of the arms is mainly based on the servomotor which is coupled with the arm through gears in order to compensate the high torque demand for rotation. This mechanism allows the movement of the whole arm around its axis as shown in Figure 2. Another servomotor is mounted in the arm which connected to the motor mount through push-pull mechanism which rotates parallel to the servo lever as shown in Figure 3. The two angles generated by the servomotors constitute towards the configuration of the rotation axes of the propellers.

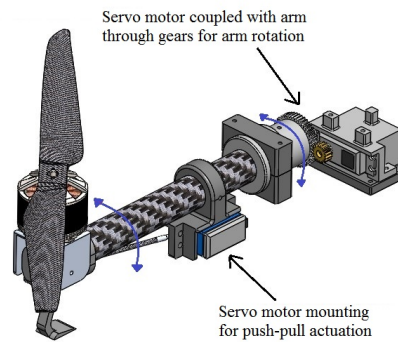


Figure 2. CAD model of proposed dual-tilting arm.

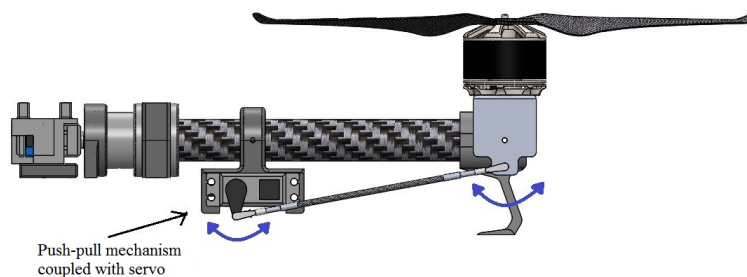


Figure 3. Push-pull mechanism for the tilting of rotor.

The gear mechanism for the coupling of servomotor with the arm of the quadcopter is installed with the gear ratio of 1:3 to fulfill the torque requirement for rotating the arm of the quadcopter. The coupling mechanism is shown in Figure 4. For the actuation of dual-axis tilting system, a total of eight servomotors are used for rotating the arms and motor mountings.

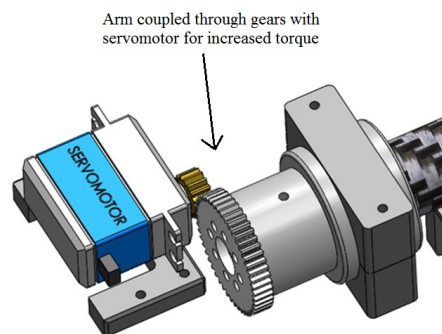


Figure 4. Gear coupling for the tilting of arm.

### 3. Modeling and Simulation of Over-Actuated Quadcopter

#### 3.1. Modeling

For the development of the mathematical model which defines the dynamics of the dual-axis tilting quadcopter, Newton-Euler formulation has been used to derive the equations. The development process includes the definition of variables and axes reference, formulation using Newton-Euler equations, and including inertia variation [29]. The inertia of the quadcopter has been considered variable due to variation of the rotors position as a result of the tilting. These dynamic equations have been developed using Maple®.

To begin the analysis of the system, three frames have been selected in order to develop the system equations. The first frame is the world frame therefore we refer to it as the frame 1 (World Frame). The next frame is defined to be fixed in the center of gravity of the UAV and is referred as frame 2 (Body Frame). Finally, the third frame is defined to be fixed in each of the rotors and is referred as frame 3 (Rotor Frame), shown in Figure 5. The overall system model diagram is shown in Figure 6. In this paper, kinematics and dynamic modeling of the dual-axis tilting system is developed (Propellers and Tilting block, shown in Figure 6), whereas the conventional quadcopter modeling details are standard text book material therefore omitted here.

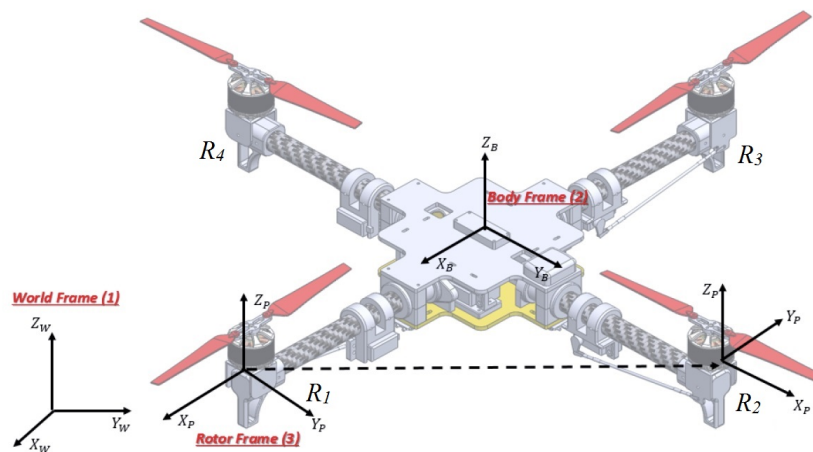


Figure 5. Rotor numbering and reference frames [29].

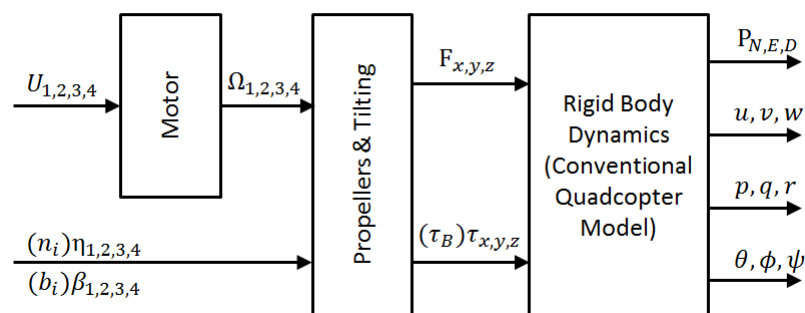


Figure 6. Dual-axis tilting quadcopter modeling diagram.

It is important to set reference frames in each rotor, to get the kinematic and dynamic equations for each rotor in the UAV. To simplify the equations, the four local frames of each rotor have been aligned with respect to the global axis following a rotational relationship with respect to the Z axis by

90° counter-clockwise. The expression which defines the rotation matrix is shown below as example of the rotation for the rotor 2.

$$\begin{bmatrix} i_2 \\ j_2 \\ k_2 \end{bmatrix}_3 = \mathbf{R}_Z\left(\frac{\pi}{2}\right) \cdot \begin{bmatrix} i_1 \\ j_1 \\ k_1 \end{bmatrix}_3$$

Similarly, the rotation matrix is applied for the rotors 3 and 4 with an angular difference of 90° counter-clockwise each, which represents 180° offset for the rotor 3 and 270° offset for the rotor 4. The general rotation matrix for each rotor therefore is defined as:

$$\begin{bmatrix} i_i \\ j_i \\ k_i \end{bmatrix}_3 = \mathbf{R}_Z\left((i-1)\frac{\pi}{2}\right) \cdot \begin{bmatrix} i_1 \\ j_1 \\ k_1 \end{bmatrix}_3 \quad \text{for } i = 1 \dots 4$$

As frame 3 is fixed, every equation is translated from frame 3 to frame 2. As result of translating the local axis of each rotor with respect to frame 2, three matrices for the rotation of each axis are obtained as  $\mathbf{R}_X$ ,  $\mathbf{R}_Y$  and  $\mathbf{R}_Z$ .

$$\mathbf{R}_X = \begin{bmatrix} 1 & 0 & 0 \\ 0 & \cos(\beta_i(t)) & -\sin(\beta_i(t)) \\ 0 & \sin(\beta_i(t)) & \cos(\beta_i(t)) \end{bmatrix} \quad (1)$$

$$\mathbf{R}_Y = \begin{bmatrix} \cos(\eta_i(t)) & 0 & \sin(\eta_i(t)) \\ 0 & 1 & 0 \\ -\sin(\eta_i(t)) & 0 & \cos(\eta_i(t)) \end{bmatrix} \quad (2)$$

$$\mathbf{R}_Z = \begin{bmatrix} \cos\left(\frac{\pi}{2} \cdot (i-1)\right) & -\sin\left(\frac{\pi}{2} \cdot (i-1)\right) & 0 \\ \sin\left(\frac{\pi}{2} \cdot (i-1)\right) & \cos\left(\frac{\pi}{2} \cdot (i-1)\right) & 0 \\ 0 & 0 & 1 \end{bmatrix}$$

Finally, the rotation matrix from frame 2 to frame 1 is obtained by three rotation matrices, one in each axis of the frame 1. In this case, the Euler angles are used to identify the orientation of the aircraft. The angles are denoted by  $\theta$ ,  $\varphi$ ,  $\psi$  corresponding to roll, pitch and yaw and representing the angular displacement of the UAV along the X, Y and Z axes respectively. The rotation matrix from the body to the fixed frame is shown in Equation (3).

$${}^2\mathbf{R}_1 = \begin{bmatrix} c(\theta)c(\psi) & -c(\theta)s(\psi) & s(\theta) \\ s(\varphi)s(\theta)c(\psi) + c(\varphi)s(\psi) & -s(\varphi)s(\theta)s(\psi) + c(\varphi)c(\psi) & -s(\varphi)c(\theta) \\ -c(\varphi)s(\theta)c(\psi) + s(\varphi)s(\psi) & c(\varphi)s(\theta)s(\psi) + s(\varphi)c(\psi) & c(\varphi)c(\theta) \end{bmatrix} \quad (3)$$

where  $c$  and  $s$  denote to the trigonometric functions *cosine* and *sine* respectively. With these equations the major problem for applying the Newton-Euler equations to our system is sorted. From this point, the calculation of the angular and linear accelerations for the UAV has been done by solving Equation (4). For the calculation of the angular accelerations, the general kinematic equation for the UAV has been used. The Equations (4) and (6) define the angular and linear accelerations of the UAV platform. The motors are rotating the propellers, this represents an angular velocity denoted by  $\Omega$ .

$$\vec{a}_B = (I_B + 4I_P)^{-1} \cdot \left[ \vec{M}_T - \sum_{i=1}^4 ({}^2\mathbf{R}_3)_i I_P \begin{pmatrix} \ddot{\beta}_i \\ \ddot{\eta}_i \\ \ddot{\Omega}_i \end{pmatrix} + ({}^2\mathbf{R}_3)_i \vec{r}_{ext} - \frac{d}{dt}(I_B)\vec{\omega}_B - \Theta I_B \vec{\omega}_B \right] \quad (4)$$

where  $\Theta$  is the Skew matrix. This is formed by the angular velocity of the platform in three axes [29], it is given as:

$$\Theta = \begin{bmatrix} 0 & -R(t) & Q(t) \\ R(t) & 0 & -P(t) \\ -Q(t) & P(t) & 0 \end{bmatrix} \quad (5)$$

$$\begin{bmatrix} \dot{u} \\ \dot{v} \\ \dot{w} \end{bmatrix} = \begin{bmatrix} 0 \\ 0 \\ -g \end{bmatrix} + \frac{1}{m} \left[ ({}^1\mathbf{R}_2) \cdot \sum_{i=1}^4 ({}^2\mathbf{R}_{3i} \cdot \vec{T}_{P_i}) \right] \quad (6)$$

Expanding these equations and considering the rotation matrices, the dynamic equations for forces and torques can be obtained as follows:

$$\begin{bmatrix} F_x \\ F_y \\ F_z \end{bmatrix} = \begin{bmatrix} (k_{x1} + \lambda_{x1}) & (k_{x2}^* + \lambda_{x2}^*) & (-k_{x3} + \lambda_{x3}) & (-k_{x4}^* - \lambda_{x4}^*) \\ (k_{x1} + \lambda_{y1}) & (k_{x2}^* + \lambda_{y2}^*) & (-k_{x3} + \lambda_{y3}) & (-k_{y4}^* - \lambda_{y4}^*) \\ (k_{z1} + \lambda_{z1}) & (k_{z2}^* + \lambda_{z4}^*) & (-k_{z3} + \lambda_{z4}) & (-k_{z4}^* - \lambda_{z4}^*) \end{bmatrix} \begin{bmatrix} T_1 \\ T_2 \\ T_3 \\ T_4 \end{bmatrix}$$

$$\begin{bmatrix} \tau_x \\ \tau_y \\ \tau_z \end{bmatrix} = \begin{bmatrix} T_x \\ T_y \\ T_z \end{bmatrix} + \begin{bmatrix} l_{xx} & l_{xy} & l_{xz} \\ l_{yx} & l_{yy} & l_{yz} \\ l_{zx} & l_{zy} & l_{zz} \end{bmatrix} \begin{bmatrix} IP_x \\ IP_y \\ IP_z \end{bmatrix} + \begin{bmatrix} \rho_x \\ \rho_y \\ \rho_z \end{bmatrix}$$

The coefficients of the forces and the torques are given in Appendix A.

It is important to mention that the inertia of the system varies due to the tilting rotors and cannot be assumed as constant (time invariant). Therefore, the inertia matrix (Equation (7)) is modeled in this paper as:

$$I_B = \begin{bmatrix} I_{xx} & 0 & 0 \\ 0 & I_{yy} & 0 \\ 0 & 0 & I_{zz} \end{bmatrix} + \begin{bmatrix} I_{P_{x'x'}} & 0 & 0 \\ 0 & I_{P_{y'y'}} & 0 \\ 0 & 0 & I_{P_{z'z''}} \end{bmatrix} + m \cdot \begin{bmatrix} y_C^2 & 0 & 0 \\ 0 & x_C^2 & 0 \\ 0 & 0 & x_C^2 + y_C^2 \end{bmatrix} \quad (7)$$

Expanding Equation (7) yields the inertia values in the main axis which are given in Appendix B.

### 3.2. Simulation

The simulation of the dynamic equations is implemented using Matlab/Simulink<sup>©</sup> incorporating the motor dynamics, attitude controller for Roll, Pitch and Yaw, and the controller for tilting angles of the rotors (Figure 7). The quadcopter can be simulated to observe the flight behaviour under the influence of different control inputs i.e. attitude commands and tilting rotor angle inputs.

Rectangular path was simulated to observe the performance of UAV using tilting angle of rotors as inputs. In Figure 8, the simulation shows the movement of UAV in a rectangular path with only using the tilting capability of the rotors without changing its attitude. The platform was able to perform sharp cornering maneuvers.

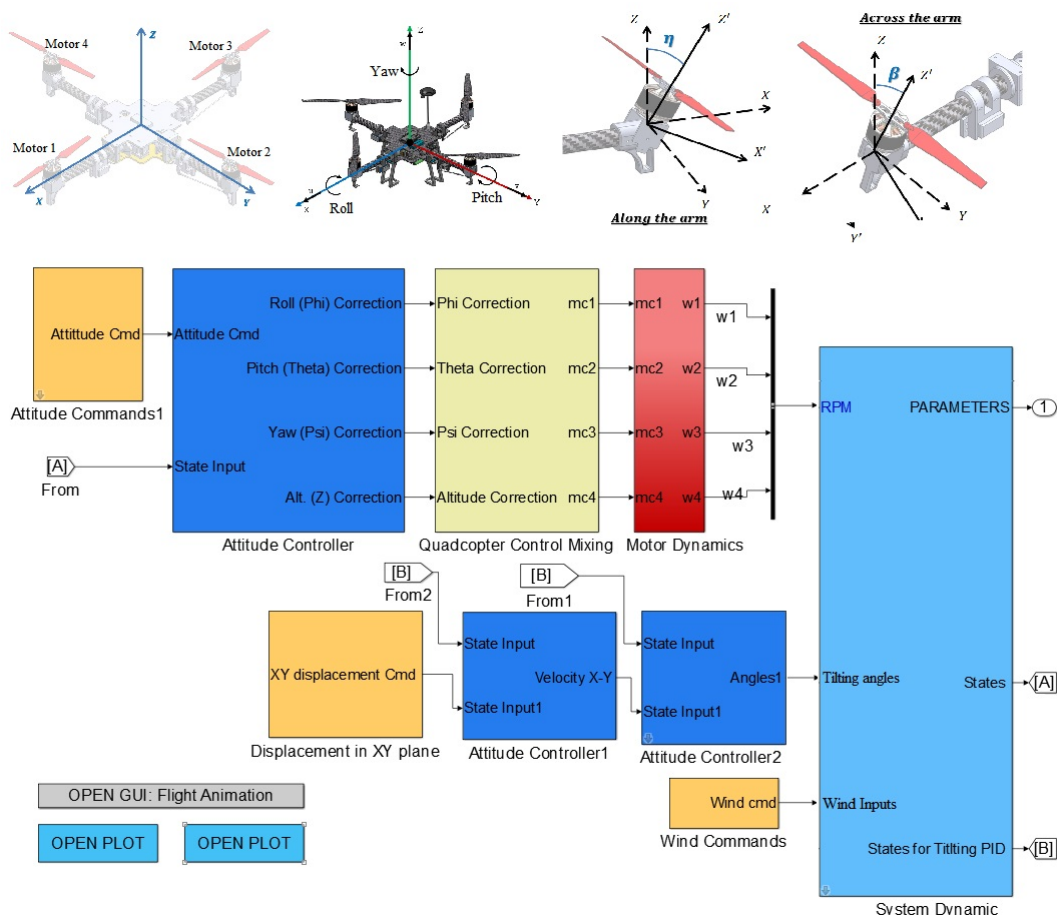


Figure 7. Simulink model.

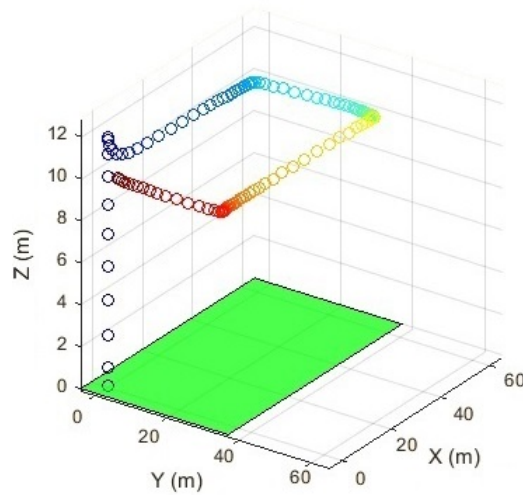
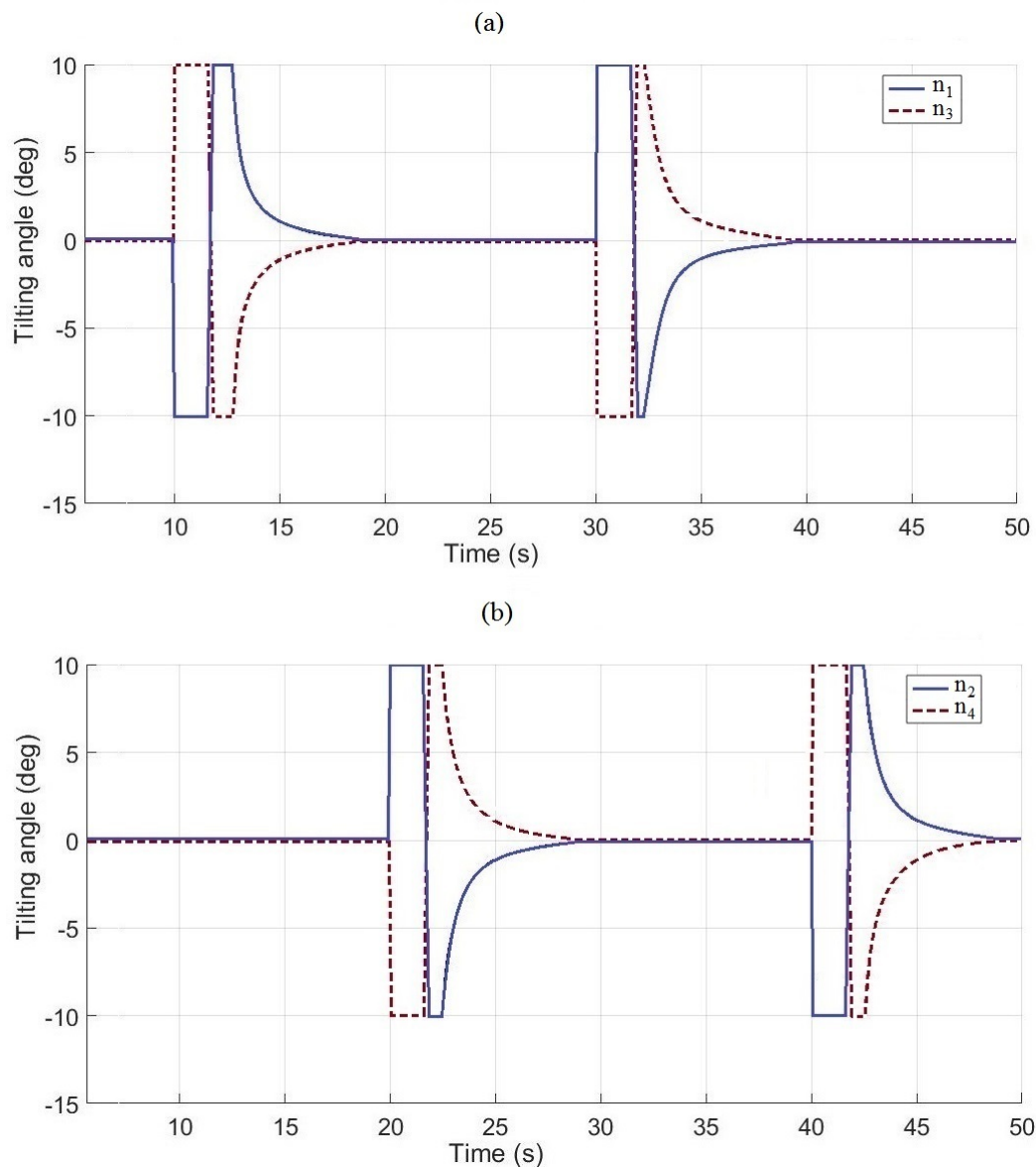


Figure 8. Rectangular path movement of UAV with tilting.

The trajectory was followed only using tilt rotor actuation. The rotor tilting angle along the arm ( $n$ ) is used to follow a rectangular trajectory. Each rotor is coupled with the opposite rotor with tilting at angles shown in Figure 9. At each corner, the adjacent rotors are tilted to follow the path. Figure 10 shows the attitude of the UAV i.e., Roll and Pitch and it can be observed that the quadcopter performs the maneuver without changing its attitude.



**Figure 9.** (a) Rotor tilting angles along the arm  $n_1$  and  $n_3$ ; (b) Rotor tilting angles along the arm  $n_2$  and  $n_4$ .

From Figure 9, rotor angles along the arm  $n_1$  and  $n_3$  are tilted at 10 degrees without a change in attitude (as observed in Figure 10) and the quadcopter starts moving in that direction. On the corners, the adjacent rotors ( $n_2$  and  $n_4$ ) are tilted to follow the trajectory.

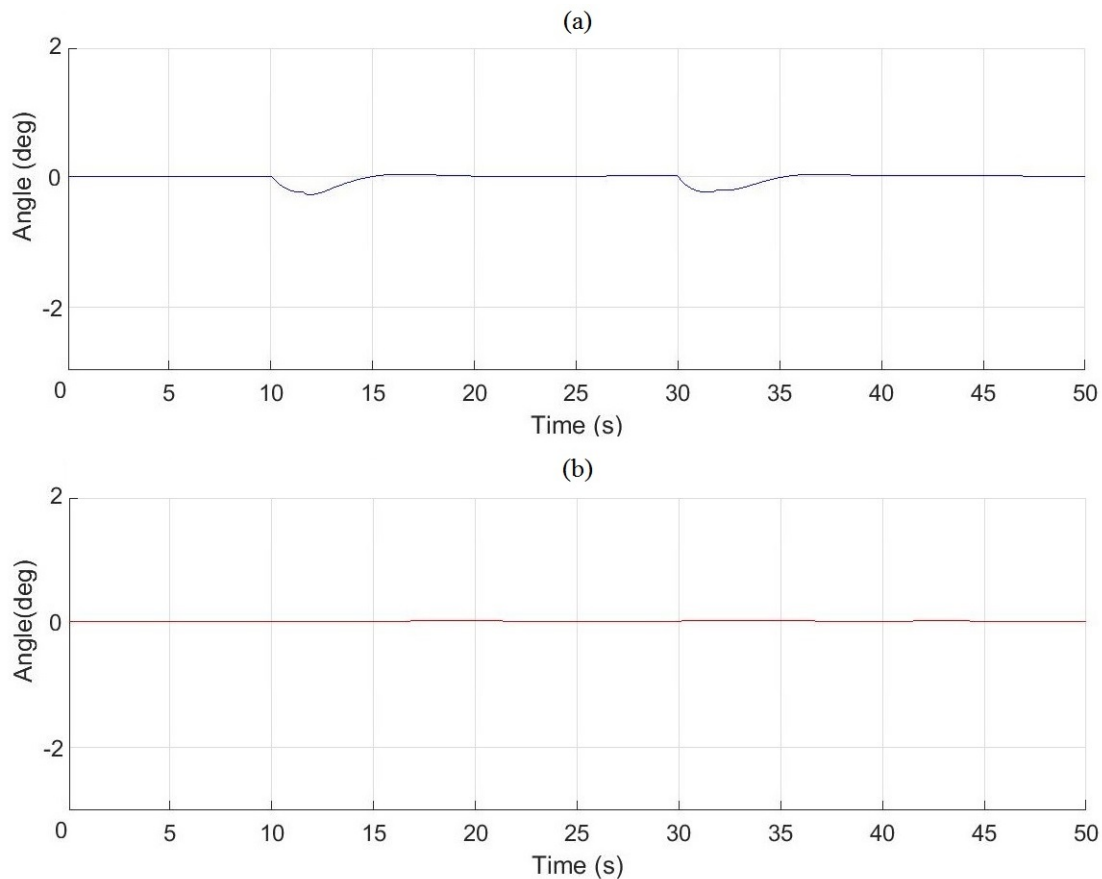


**Figure 10.** (a) Roll angle of the UAV; (b) Pitch angle of the UAV.

#### 4. Experimental Setup

The four brushless motors selected were the Tiger T-MOTOR MN4014-9 400Kv with a 2-blade  $15 \times 5$  Carbon Fiber propellers as shown in Figure 11.



**Figure 11.** (Left) Brushless motor; (Right) Propeller used for thrust generation.

For the Flight Control of the UAV, ArduPilotMega (APM) was used. APM is an open-source flight controller, able to control autonomous multicopters, fixed-wing aircraft, traditional helicopters and ground rovers. It is based on the Arduino electronics prototyping platform. Apart from the APM, which is mainly controlling the brushless motors and handling the inner loop control of the vehicle, the Arduino Leonardo microcontroller board is used to control the added servomotors. Figure 12 show the controllers used for the proposed vehicle.

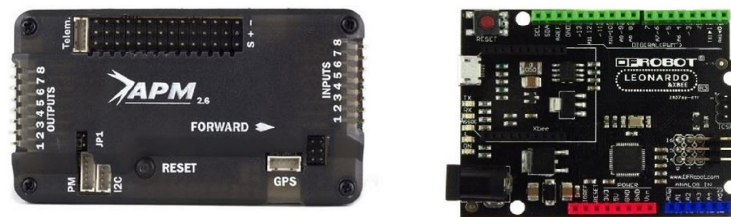


Figure 12. (Left) APM Flight controller; (Right) Arduino Leonardo.

The inner-loop control of the quadcopter is handled by the APM. This on-board inner-loop control device deals with control and stabilization required to hover and perform basic maneuvers. The APM board contains the inertial sensors required for the orientation and heading determination and its software includes the inner-loop control algorithm and the basic Graphical User Interface (GUI) for visualization. Generally, the APM input is provided by the RC remote control which allows the user to manually control and fly the multicopter. The TGY-i10 RC Controller was used as the input for the flight controller. GPS module was attached to the APM in order to navigate the aircraft and track its position for post-processing and analysis. The APM attitude controller was fused with the other controller which was aimed for controlling the inputs for the servo motors responsible for the tilting of the rotors. This controller mainly controls the tilting of the servomotors by combining the inputs for the attitude control of the UAV and the tilting commands for the rotors from the pilot. The commands generated by the human pilot using RC Controller are received by the Arduino Leonardo. The pilot has control of the conventional attitude of quadcopter and tilting servomotors. Based on the control inputs from the pilot, Arduino reads in Pulse Position Modulation (PPM) signals from the RC controller and generates commands (PPM signals) of roll, pitch, yaw and throttle to the APM and commands for servomotors simultaneously. This allows the pilot to have full control of all the actuators of the dual-tilting quadcopter. If the pilot wants to perform maneuvers using only tilting, the Arduino generates commands for the servo motors and proportionally generates attitude commands in order to compensate the tilting actuation.

Currently the tilting angle is limited to  $10^\circ$  for each servomotor. Unlike the conventional quadcopter, this gives the pilot additional control inputs i.e., tilting of the rotors along with conventional control for increased maneuverability. The altitude during all the flight tests was kept in altitude hold mode. The APM flight controller provides the feature of holding the altitude allowing to hover and maneuver at the desired altitude.

The control implementation here is rather basic since a more sophisticated development is out of the scope of this paper but remains in the future work agenda. The conventional inner loop controller of the APM [30] allows the quadcopter to respond to attitude commands of the pilot which are passed through Arduino Leonardo. Arduino Leonardo allows the control of the attitude and the tilting simultaneously. Figure 13 illustrates the experimental setup for control.

After assembling all the manufactured parts and integrating the related modules for the over-actuated mechanisms for the quadcopter, the final product is shown in Figure 14.

Table 1 presents some of the technical specifications of the developed quadcopter.

Table 1. UAV Technical Specifications.

| Parameter        | Specifications        |
|------------------|-----------------------|
| UAV Dimensions   | $1048 \times 1048$ mm |
| Weight           | 4 kg                  |
| Endurance        | 20 min                |
| Payload Capacity | 2 kg                  |

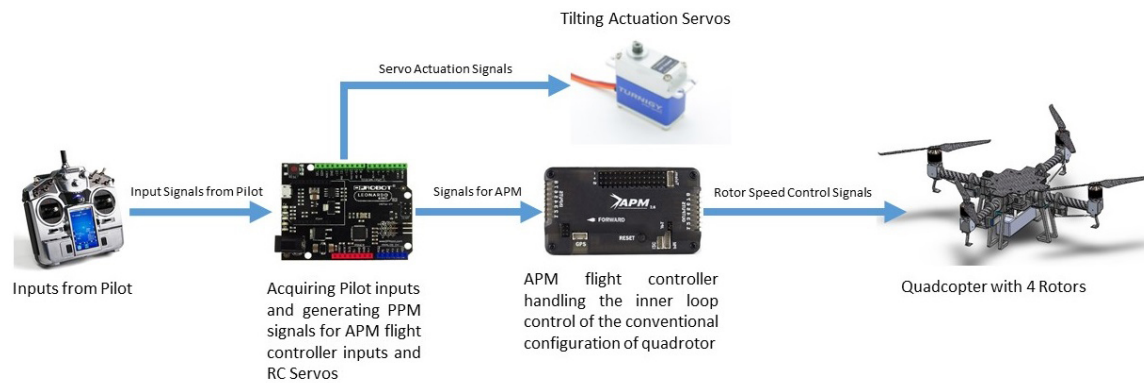


**Figure 13.** Experimental setup for control of the UAV.



**Figure 14.** Dual-tilting quadcopter prototype.

## 5. Results and Discussion

### 5.1. Flight Test with Conventional Actuation of Quadcopter

After the successful manufacturing and assembly of the vehicle, flight test was conducted for the conventional under-actuated configuration of the quadcopter in order to validate the design parameters and the dynamic model of the vehicle. Relevant flight variables of interest were analyzed in order to observe the behaviour and attitude for the designed vehicle. The results in Figures 15–17 show the control of each axis.

For each axis, the vehicle performs satisfactorily and flies according to the input angles given by the pilot through RC control. GPS is used for the position feedback as ground truth. The proposed system performs well for the conventional configuration and flight controls and validates the design of the platform and its flight stability for the conventional control. Therefore, it can be concluded that the vehicle is stable and able to maintain its attitude. Moreover, the platform can be used for developing and testing of the flight controls for the over-actuated configuration and performs well with proper control techniques for the over-actuated quadcopter design. With the development of over-actuated quadcopter controller, the manufactured vehicle gives plenty of control authority and high maneuverability due to its capability to incorporate the excess number of control inputs.

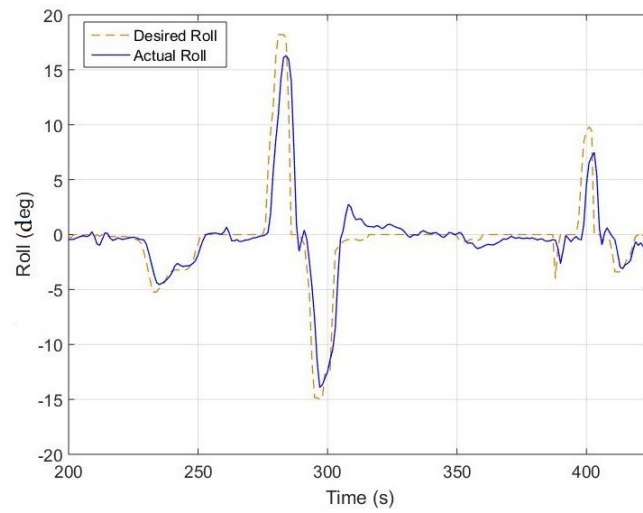


**Figure 15.** Roll command tracking of the vehicle.

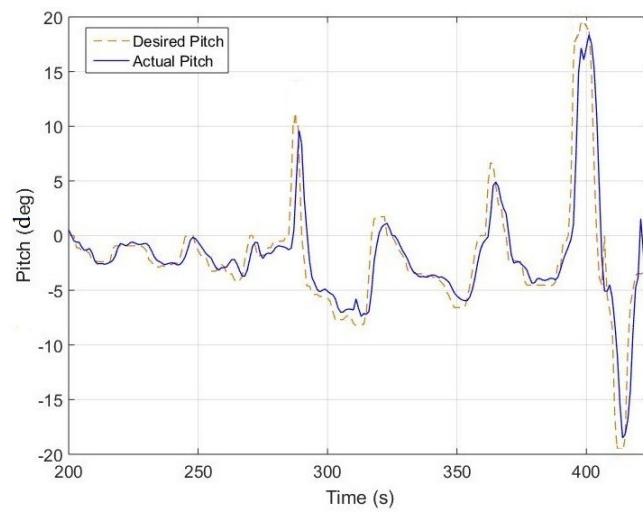


**Figure 16.** Pitch command tracking of the vehicle.

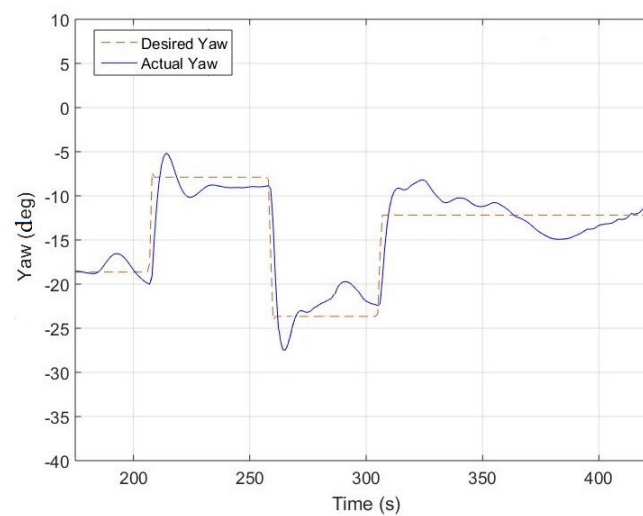


**Figure 17.** Yaw command tracking of the vehicle.

## 5.2. Flight Test with Tilting Rotors

The experimental scenario was created in order to validate the performance of the quadcopter using tilting rotors. As mentioned in Section 3, the quadcopter was simulated to imitate a rectangular trajectory which involves sharp cornering for the vehicle. Real corners (imitating trees in a dense forest) were created in an outdoor flying space, the quadcopter was flown to follow the rectangular trajectory along those corners with tilting and without tilting rotors. Figure 18 shows the track followed by the quadcopter using only tilting angles.

The attitude of the quadcopter during the flight can be observed in Figure 19 which shows that the quadcopter is stabilizing and maintaining its horizontal attitude without contributing in the movement in order to follow the trajectory. The rectangular trajectory including the cornering is achieved using only tilting of the rotors along the arms.

The same trajectory following was performed without using tilting of the rotors, with conventional configuration of the quadcopter. The results of trajectory followed by the quadcopter with conventional configuration is shown in Figure 20.

Comparing of the quadcopter attitude in both cases, i.e. with conventional actuation and with tilting rotor actuation for the same trajectory (Figures 19 and 21), it can be observed that the quadcopter with conventional actuation requires the whole frame to be tilted in order to maintain attitude. Whereas dual tilting actuation quadcopter provides the ability to maneuver in a way regardless of its attitude.

Furthermore, it is evident from the comparison of the trajectory followed by the quadcopter with two different actuation strategies that the quadcopter with tilting actuation of the rotors is able to maneuver efficiently through corners which minimizes the effort of the vehicle movement.

From Figures 18 and 20, it can be noticed that the conventional actuation of the quadcopter limits the motion of the vehicle around sharp corners up to certain extent, requiring a larger turning radius in order to do the cornering. The clearing distance through obstacles using tilting is  $d = 1.25$  m, while with the conventional configuration,  $d = 2.65$  m. It is clear that wider gap is required for the conventional quadcopter to fly through the obstacles whereas with tilting ability, the quadcopter is able to fly more precisely, reducing the clearing distance. The conventional quadcopter would not be able to execute such maneuvers as the under-actuation limits its ability. Tilting provides more controllability and ability to the vehicle as it can move without changing its attitude which helps the developed system to fly through narrow gaps and under trees canopy. The combination of tilting rotors with attitude control provide increased agility and control bandwidth in an urban outdoor scenario where the flying through narrow gaps and obstacles is challenging as compared to under-actuated quadcopter.

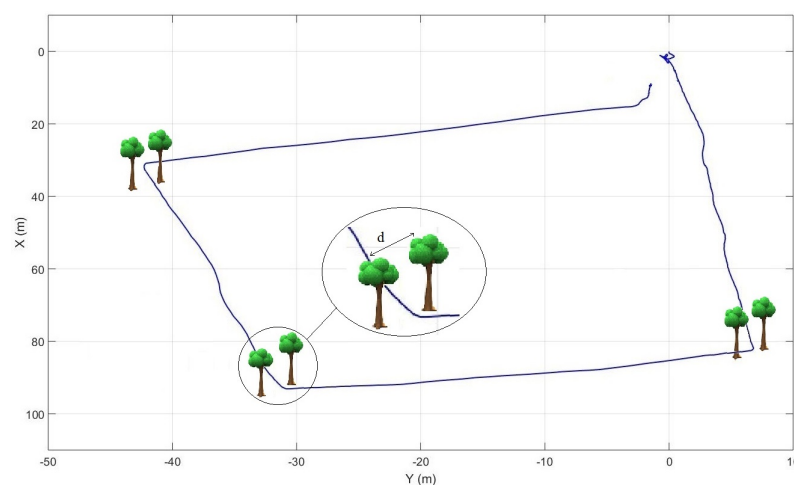


**Figure 18.** The real-time trajectory followed by UAV using tilting,  $d = 1.25$  m.

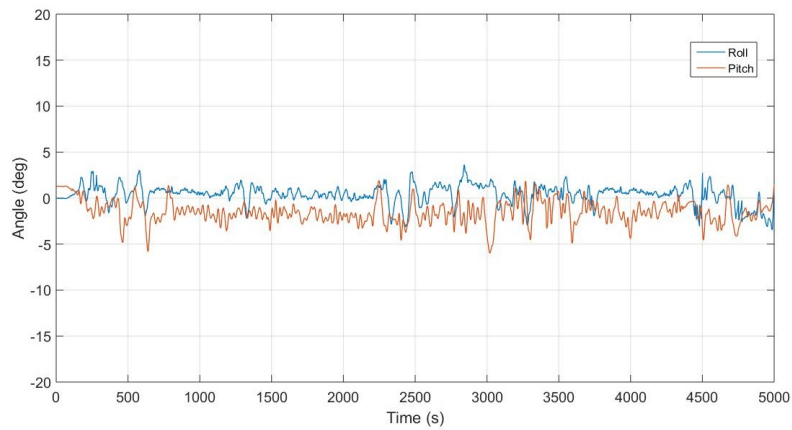


Figure 19. Roll and pitch angle of the UAV while maneuvering only with tilting.

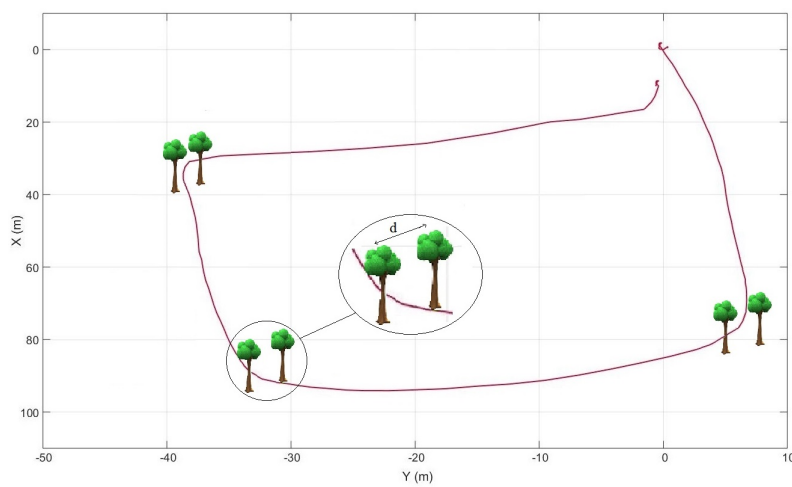


Figure 20. The real-time trajectory followed by UAV without using tilting,  $d = 2.65$  m.

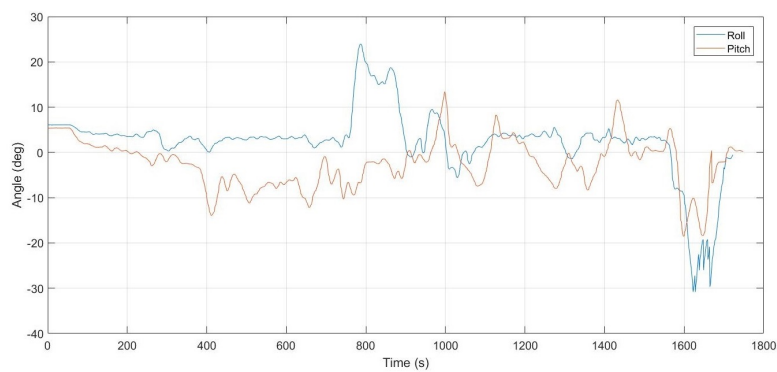


Figure 21. Roll and Pitch angle of the UAV while maneuvering without tilting.

## 6. Conclusions

This paper proposes a design and implementation of an over-actuated quadcopter with dual-axis tilting rotors. The CAD model was developed following the manufacturing of the system using rapid prototyping in order to minimize the manufacturing time and cost. The modeling and simulation of the over-actuated system allowed observing the behavior of the platform using different control inputs. The flight test results in outdoor conditions show satisfactory performance of the developed platform.

The experiments were performed to observe and compare the capability of over-actuated configuration against conventional configuration which showed that the proposed platform performs better when it comes to flying along corners and between adjacent obstacles, and gives better maneuverability compared to conventional quadcopter.

Integration of dual-axis tilting capability to quadcopters opens different research areas, including developing control and recovery strategies. Quadcopter with dual-tilting actuation will vastly expand its applications in search and rescue missions, detecting missing persons in a wide dense forest area with advantage of being able to fly under trees canopy.

Future work will focus on quantifying the energy consumption and the development of different fail-safe strategies in case of failure of one or two of the rotors. The development of failure strategies will use the full capability of over-actuation presented in the current research.

**Author Contributions:** All authors have made great contributions to the work. A.B.J., J.B.B. and Y.Z. designed and built the platform. A.D.D.C.S., J.B.B. and Y.Z. developed the model and the simulation. A.B.J., A.D.D.C.S. and N.V. conducted the experiments. A.B.J., N.V. and Y.Z. analyzed the data and revised the manuscript.

**Funding:** This research received no external funding.

**Acknowledgments:** The authors would like to thank Miguel Guzman and Zineb Chelh for their help in the preliminary platform design and simulation.

**Conflicts of Interest:** The authors declare no conflict of interest.

## Abbreviations

The following abbreviations are used in this manuscript:

|                    |   |
|--------------------|---|
| $\theta$           | Pitch angle                             |
| $\varphi$          | Roll angle                              |
| $\psi$             | Yaw angle                               |
| $\omega_i$         | Angular velocity                        |
| $L$                | Arm length                              |
| $dIB_x$            | Time derivative of inertia along X axis |
| $dIB_y$            | Time derivative of inertia along Y axis |
| $dIB_z$            | Time derivative of inertia along Z axis |
| $IB_{xx}$          | Body's inertia along X axis             |
| $IB_{yy}$          | Body's inertia along Y axis             |
| $IB_{zz}$          | Body's inertia along Z axis             |
| $IP_x$             | Propeller's inertia along X axis        |
| $IP_y$             | Propeller's inertia along Y axis        |
| $IP_z$             | Propeller's inertia along Z axis        |
| $i$                | number of rotor (1, 2, 3, 4)            |
| $P_{N,E,D}$        | Position in North, East and Down axis   |
| $P$                | Angular velocity in X axis              |
| $Q$                | Angular velocity in Y axis              |
| $R$                | Angular velocity in Z axis              |
| $n_i$ or $\eta_i$  | Rotor tilting angle along the arm       |
| $b_i$ or $\beta_i$ | Rotor tilting angle across the arm      |
| $x_W, y_W, z_W$    | Fixed frame (1)                         |
| $x_B, y_B, z_B$    | Body frame (2)                          |
| $x_P, y_P, z_P$    | Rotor frame (3)                         |
| $R_x, R_y, R_z$    | Rotation matrices in x, y and z axis    |
| $\alpha$           | Angular acceleration                    |
| $u, v, w$          | Linear velocity in x, y and z axis      |
| $T_i$              | Thrust generated by the rotor $i$       |

## Appendix A. Coefficients of the Forces and the Torques

The coefficients of the force dynamic equation in  $x$ -axis are as follows:

$$k_{xi} = \sin(\phi) \sin(\theta) [\cos(b_i) [\sin(n_i) \cos(\psi) - \cos(n_i)] - \sin(b_i) \sin(\psi)] \quad (\text{A1})$$

$$k_{xi}^* = \sin(\phi) \sin(\theta) [\cos(b_i) [\sin(n_i) \cos(\psi) + \cos(n_i)] + \sin(b_i) \sin(\psi)] \quad (\text{A2})$$

$$\lambda_{xi} = \cos(\theta) [\sin(b_i) \cos(\psi) + \sin(n_i) \cos(b_i) + \sin(\psi)] \quad (\text{A3})$$

$$\lambda_{xi}^* = \cos(\theta) [\sin(b_i) \cos(\psi) - \sin(n_i) \cos(b_i) + \sin(\psi)] \quad (\text{A4})$$

The coefficients of the force dynamic equation in  $y$ -axis are as follows:

$$k_{yi} = \sin(\phi) \sin(\theta) [\cos(b_i) [\sin(n_i) \cos(\psi) + \cos(n_i)] - \sin(b_i) \sin(\psi)] \quad (\text{A5})$$

$$k_{yi}^* = \sin(\phi) \sin(\theta) [\cos(b_i) [\sin(n_i) \cos(\psi) - \cos(n_i)] + \sin(b_i) \sin(\psi)] \quad (\text{A6})$$

$$\lambda_{yi} = \cos(\phi) [\sin(b_i) \cos(\psi) + \sin(n_i) \cos(b_i) \sin(\psi)] \quad (\text{A7})$$

$$\lambda_{yi} = \cos(\phi) [\sin(b_i) \cos(\psi) + \sin(n_i) \cos(b_i) \sin(\psi)] \quad (\text{A8})$$

The coefficients of the force dynamic equation in  $z$ -axis are as follows:

$$k_{z1} = \sin(\theta) [\sin(\psi) [\sin(n_1) \cos(b_1) - \sin(b_1) \cos(\phi)] - \sin(n_1) \cos(b_1) \cos(\phi) \cos(\psi)] \quad (\text{A9})$$

$$k_{z2} = \sin(\theta) [\sin(\psi) [\sin(b_2) + \sin(n_2) \cos(b_2) \cos(\phi)] - \sin(b_2) \cos(\phi) \cos(\psi)] \quad (\text{A10})$$

$$k_{z3} = -\sin(\theta) [\sin(\psi) [\sin(n_3) \cos(b_3) + \sin(b_3) \cos(\phi)] - \sin(n_3) \cos(b_3) \cos(\phi) \cos(\psi)] \quad (\text{A11})$$

$$k_{z4} = \sin(\theta) [\sin(\psi) [\sin(b_4) + \sin(n_4) \cos(b_4) \cos(\phi)] - \sin(b_4) \cos(\phi) \cos(\psi)] \quad (\text{A12})$$

$$\lambda_{z1} = \cos(n_1) \cos(b_1) \cos(\theta) \cos(\phi) - \sin(b_1) \sin(\phi) \cos(\psi) \quad (\text{A13})$$

$$\lambda_{z2} = \cos(b_2) [\sin(n_2) \sin(\phi) \cos(\psi) - \cos(n_2) \cos(\phi) \cos(\theta)] \quad (\text{A14})$$

$$\lambda_{z3} = -\cos(n_3) \cos(b_3) \cos(\theta) \cos(\phi) + \sin(b_1) \sin(\phi) \cos(\psi) \quad (\text{A15})$$

$$\lambda_{z4} = -\cos(b_4) [\sin(n_4) \sin(\phi) \cos(\psi) - \cos(n_4) \cos(\phi) \cos(\theta)] \quad (\text{A16})$$

The coefficients of the torque dynamic equation in  $x$ -axis are as follows:

$$l_{xx} = -\cos(n_1) IP_x \ddot{b}_1 - \sin(n_2) \sin(b_2) IP_x \ddot{b}_2 + \cos(n_3) IP_x \ddot{b}_3 + \sin(n_4) \sin(b_4) IP_x \ddot{b}_4 \quad (\text{A17})$$

$$l_{xy} = -\sin(n_1) \sin(b_1) IP_y \ddot{n}_1 + \cos(b_2) IP_y \ddot{n}_2 + \sin(n_3) \sin(b_3) IP_y \ddot{n}_3 - \cos(b_4) IP_y \quad (\text{A18})$$

$$l_{xz} = -\sin(n_1) \cos(b_1) IP_z \omega_1 - \sin(b_2) IP_z \omega_2 + \sin(n_3) \cos(b_3) IP_z \omega_3 + \sin(b_4) IP_z \omega_4 \quad (\text{A19})$$

$$\rho_x = QRIB_{yy} - QRIB_{zz} - PdIB_x \quad (\text{A20})$$

The coefficients of the torque dynamic equation in  $y$ -axis are as follows:

$$l_{yx} = \sin(n_1) \sin(b_1) IP_x \ddot{b}_1 - \sin(n_2) IP_x \ddot{b}_2 - \sin(n_3) \sin(b_3) IP_x \ddot{b}_3 + \sin(n_4) IP_x \ddot{b}_4 \quad (\text{A21})$$

$$I_{yy} = -\cos(b_1)IP_y\ddot{n}_1 - \sin(n_2)\sin(b_2)IP_y\ddot{n}_2 + \cos(b_3)IP_y\ddot{n}_3 + \sin(n_4)\sin(b_4)IP_y\ddot{n}_4 \tag{A22}$$

$$I_{yz} = \sin(b_1)IP_z\omega_1 - \sin(n_2)\cos(b_2)IP_z\omega_2 - \sin(b_3)IP_z\omega_3 + \sin(n_4)\cos(b_4)IP_z\omega_4 \tag{A23}$$

$$\rho_y = PRIB_{zz} - PRIB_{xx} - QdIB_y \tag{A24}$$

The coefficients of the torque dynamic equation in z-axis are as follows:

$$I_{zx} = \sin(n_1)IP_x\ddot{b}_1 + \sin(n_2)IP_x\ddot{b}_2 + \sin(n_3)IP_x\ddot{b}_3 + \sin(n_4)IP_x\ddot{b}_4 \tag{A25}$$

$$I_{zy} = -\cos(n_1)\sin(b_1)IP_y\ddot{n}_1 - \cos(n_2)\sin(b_2)IP_y\ddot{n}_2 - \cos(n_3)\sin(b_3)IP_y\ddot{n}_3 - \cos(n_4)\sin(b_4)IP_y\ddot{n}_4 \tag{A26}$$

$$I_{zz} = \cos(n_1)\cos(b_1)IP_z\omega_1 + \cos(n_2)\cos(b_2)IP_z\omega_2 + \cos(n_3)\cos(b_3)IP_z\omega_3 + \cos(n_4)\cos(b_4)IP_z\omega_4 \tag{A27}$$

$$\rho_z = QPIB_{xx} - PQIB_{yy} - RdIB_z \tag{A28}$$

### Appendix B. Inertia Values

Expanding Equation (7) yields the inertia values in the main axis as follows:

$$I_{Bxx} = I_{xx} + 2I_{Pxx} + 2I_{Pzz} + \lambda [\cos(2\eta_1) + \cos(2\eta_2) + \cos(2\eta_3) + \cos(2\eta_4)] + 2m_pL^2 \tag{A29}$$

$$I_{Byy} = I_{yy} + 2I_{Pyy} + I_{Pxx} + I_{Pzz} - \frac{1}{2}\lambda [\cos(2\eta_1) + \cos(2\eta_2) + \cos(2\eta_3) + \cos(2\eta_4)] + \zeta [\cos(2\beta_1) + \cos(2\beta_2) + \cos(2\beta_3) + \cos(2\beta_4)] + \frac{1}{2}\lambda [\cos(2\eta_1)\cos(2\beta_1) + \cos(2\eta_2)\cos(2\beta_2) + \cos(2\eta_3)\cos(2\beta_3) + \cos(2\eta_4)\cos(2\beta_4)] + 2m_pL^2 \tag{A30}$$

$$I_{Bzz} = I_{zz} + 2I_{Pyy} + I_{Pxx} + I_{Pzz} - \frac{1}{2}\lambda [\cos(2\eta_1) + \cos(2\eta_2) + \cos(2\eta_3) + \cos(2\eta_4)] - \zeta [\cos(2\beta_1) + \cos(2\beta_2) + \cos(2\beta_3) + \cos(2\beta_4)] - \frac{1}{2}\lambda [\cos(2\eta_1)\cos(2\beta_1) + \cos(2\eta_2)\cos(2\beta_2) + \cos(2\eta_3)\cos(2\beta_3) + \cos(2\eta_4)\cos(2\beta_4)] + 4m_pL^2 \tag{A31}$$

where the value of  $\zeta$  and  $\lambda$  are defined as follows

$$\lambda = \frac{1}{2}(I_{Pxx} - I_{Pzz}) \tag{A32}$$

$$\zeta = \frac{1}{2}I_{Pyy} - \frac{1}{4}I_{Pxx} - \frac{1}{4}I_{Pzz}$$

The last expression to be derived is the time derivative of the inertia matrix which is given by Equations (A29)–(A31). For each principal axis of the inertia, it yields:

$$\frac{d}{dt}(I_{Bxx}) = -2\lambda \left( \sin(2\eta_1) \left( \frac{d}{dt}(\eta_1) \right) \right) - 2\lambda \left( \sin(2\eta_2) \left( \frac{d}{dt}(\eta_2) \right) \right) - 2\lambda \left( \sin(2\eta_3) \left( \frac{d}{dt}(\eta_3) \right) \right) - 2\lambda \left( \sin(2\eta_4) \left( \frac{d}{dt}(\eta_4) \right) \right) \tag{A33}$$

$$\begin{aligned}
\frac{d}{dt}(I_B yy) = & \lambda \sin(2\eta_1) \frac{d}{dt}(\eta_1) + \lambda \sin(2\eta_2) \frac{d}{dt}(\eta_2) + \lambda \sin(2\eta_3) \frac{d}{dt}(\eta_3) \\
& + \lambda \sin(2\eta_4) \frac{d}{dt}(\eta_4) - \lambda \sin(2\eta_1) \cos(2\beta_1) \frac{d}{dt}(\eta_1) - \lambda \sin(2\eta_2) \cos(2\beta_2) \frac{d}{dt}(\eta_2) \\
& - \lambda \sin(2\eta_3) \cos(2\beta_3) \frac{d}{dt}(\eta_3) - \lambda \sin(2\eta_4) \cos(2\beta_4) \frac{d}{dt}(\eta_4) \\
& - 2 \left( \zeta + \frac{1}{2} \lambda \cos(2\eta_1) \right) \sin(2\beta_1) \frac{d}{dt}(\beta_1) - 2 \left( \zeta + \frac{1}{2} \lambda \cos(2\eta_2) \right) \sin(2\beta_2) \frac{d}{dt}(\beta_2) \\
& - 2 \left( \zeta + \frac{1}{2} \lambda \cos(2\eta_3) \right) \sin(2\beta_3) \frac{d}{dt}(\beta_3) - 2 \left( \zeta + \frac{1}{2} \lambda \cos(2\eta_4) \right) \sin(2\beta_4) \frac{d}{dt}(\beta_4)
\end{aligned} \tag{A34}$$

$$\begin{aligned}
\frac{d}{dt}(I_B zz) = & \lambda \sin(2\eta_1) \frac{d}{dt}(\eta_1) + \lambda \sin(2\eta_2) \frac{d}{dt}(\eta_2) + \lambda \sin(2\eta_3) \frac{d}{dt}(\eta_3) \\
& + \lambda \sin(2\eta_4) \frac{d}{dt}(\eta_4) + \lambda \sin(2\eta_1) \cos(2\beta_1) \frac{d}{dt}(\eta_1) + \lambda \sin(2\eta_2) \cos(2\beta_2) \frac{d}{dt}(\eta_2) \\
& + \lambda \sin(2\eta_3) \cos(2\beta_3) \frac{d}{dt}(\eta_3) + \lambda \sin(2\eta_4) \cos(2\beta_4) \frac{d}{dt}(\eta_4) \\
& + 2 \left( \zeta + \frac{1}{2} \lambda \cos(2\eta_1) \right) \sin(2\beta_1) \frac{d}{dt}(\beta_1) + 2 \left( \zeta + \frac{1}{2} \lambda \cos(2\eta_2) \right) \sin(2\beta_2) \frac{d}{dt}(\beta_2) \\
& + 2 \left( \zeta + \frac{1}{2} \lambda \cos(2\eta_3) \right) \sin(2\beta_3) \frac{d}{dt}(\beta_3) + 2 \left( \zeta + \frac{1}{2} \lambda \cos(2\eta_4) \right) \sin(2\beta_4) \frac{d}{dt}(\beta_4)
\end{aligned} \tag{A35}$$

## References

1. Mahony, R.; Kumar, V. Aerial Robotics and the Quadrotor. *IEEE Robot. Autom. Mag.* **2012**, *19*, 19. [[CrossRef](#)]
2. Doherty, P.; Rudol, P. A UAV Search and Rescue Scenario with Human Body Detection and Geolocalization. In Proceedings of the Australian Conference on Artificial Intelligence, Gold Coast, Australia, 2–6 December 2007; pp. 1–13. [[CrossRef](#)]
3. Mahony, R.; Kumar, V.; Corke, P. Multirotor Aerial Vehicles: Modeling, Estimation, and Control of Quadrotor. *IEEE Robot. Autom. Mag.* **2012**, *19*, 20–32. [[CrossRef](#)]
4. Hua, M.D.; Hamel, T.; Morin, P.; Samson, C. A Control Approach for Thrust-Propelled Underactuated Vehicles and its Application to VTOL Drones. *IEEE Trans. Autom. Control* **2009**, *54*, 1837–1853.
5. Hua, M.D.; Hamel, T.; Morin, P.; Samson, C. Introduction to feedback control of underactuated VTOL vehicles: A review of basic control design ideas and principles. *IEEE Control Syst.* **2013**, *33*, 61–75. [[CrossRef](#)]
6. Lo, C.H.; Shin, H.S.; Tsourdos, A.; Kim, S. Modeling and Simulation of Fault Tolerant Strategies for A Quad Rotor UAV. In Proceedings of the AIAA Modeling and Simulation Technologies Conference, Minneapolis, MI, USA, 13–16 August 2012.
7. Morozov, Y.V. Emergency Control of a Quadcopter in Case of Failure of Two Symmetric Propellers. *Autom. Remote Control* **2018**, *79*, 463–478. [[CrossRef](#)]
8. Adir, V.G.; Stoica, A.M.; Marks, A.; Whidborne, J.F. stabilization and single motor failure recovery of a 4Y octorotor. In Proceedings of the IASTED International Conference on Intelligent Systems and Control (ISC 2011), Cambridge, UK, 11–13 July 2011; pp. 82–87.
9. Michieletto, G.; Ryll, M.; Franchi, A. Control of statically hoverable multi-rotor aerial vehicles and application to rotor-failure robustness for hexarotors. In Proceedings of the 2017 IEEE International Conference on Robotics and Automation (ICRA), Singapore, 29 May–3 June 2017; pp. 2747–2752. [[CrossRef](#)]
10. Cutler, M.; Ure, N.K.; Michini, B.; How, J. Comparison of Fixed and Variable Pitch Actuators for Agile Quadrotors. In Proceedings of the AIAA Guidance, Navigation, and Control Conference, Portland, OR, USA, 8–11 August 2011.
11. Oner, K.T.; Cetinsoy, E.; Unel, M.; Aksit, M.F.; Kandemir, I.; Gulez, K. Dynamic model and control of a new quadrotor unmanned aerial vehicle with tilt-wing mechanism. *World Acad. Sci. Eng. Technol.* **2008**, *45*, 58–63.
12. Jiang, G.; Voyles, R. Hexrotor UAV platform enabling dextrous interaction with structures-flight test. In Proceedings of the 2013 IEEE International Symposium on Safety, Security, and Rescue Robotics (SSRR), Linköping, Sweden, 21–26 October 2013; pp. 1–6. [[CrossRef](#)]
13. Gasco, P.S. Development of a Dual Axis Tilt Rotorcraft. Master's Thesis, Cranfield University, Bedford, UK, 2012.
14. Gasco, P.S.; Al-Rihani, Y.; Shin, H.S.; Savvaris, A. A novel actuation concept for a multi rotor UAV. In Proceedings of the International Conference on Unmanned Aircraft Systems (ICUAS), Atlanta, GA, USA, 28–31 May 2013; pp. 373–382. [[CrossRef](#)]
15. Nemati, A.; Kumar, M. Modeling and control of a single axis tilting quadcopter. In Proceedings of the American Control Conference, Portland, OR, USA, 4–6 June 2014; pp. 3077–3082. [[CrossRef](#)]

16. Scholz, G.; Trommer, G.F. Model based control of a quadrotor with tiltable rotors. *Gyrosc. Navig.* **2016**, *7*, 72–81. [[CrossRef](#)]
17. Lim, K.; Shin, J.Y.; Moerder, D.; Cooper, E. A New Approach to Attitude Stability and Control for Low Airspeed Vehicles. In Proceedings of the AIAA Guidance, Navigation, and Control Conference, Providence, RI, USA, 16–19 August 2004. [[CrossRef](#)]
18. Gress, G. Using Dual Propellers as Gyroscopes for Tilt-Prop Hover Control. In Proceedings of the Biennial International Powered Lift Conference and Exhibit, Williamsburg, VA, USA, 5–7 November 2002.
19. Gress, G. Lift fans as gyroscopes for controlling compact VTOL air vehicles: Overview and development status of Oblique Active Tilting. In Proceedings of the American Helicopter Society 63th Annual Forum, Virginia Beach, VA, USA, 1–3 May 2007.
20. Sanchez, A.; Escareño, J.; Garcia, O.; Lozano, R. Autonomous Hovering of a Noncyclic Tiltrotor UAV: Modeling, Control and Implementation. *IFAC Proce. Vol.* **2008**, *41*, 803–808. [[CrossRef](#)]
21. Klippstein, H.; Diaz De Cerio Sanchez, A.; Hassanin, H.; Zweiri, Y.; Seneviratne, L. Fused Deposition Modeling for Unmanned Aerial Vehicles (UAVs): A Review. *Adv. Eng. Mater.* **2017**, 1700552. [[CrossRef](#)]
22. Klippstein, H.; Hassanin, H.; Diaz De Cerio Sanchez, A.; Zweiri, Y.; Seneviratne, L. Additive Manufacturing of Porous Structures for Unmanned Aerial Vehicles Applications. *Adv. Eng. Mater.* **2018**, 1800290. [[CrossRef](#)]
23. Pragada, L.K.D.; Katukam, R. 3d printing of quadcopter: A Case Study. *Int. J. Latest Trends Eng. Technol.* **2015**, *5*, 131–140.
24. Hooi, C.G. Design, Rapid Prototyping and Testing of a Ducted Fan Microscale Quadcopter. In Proceedings of the American Helicopter Society 70th Annual Forum, Montreal, QC, Canada, 20–22 May 2014.
25. Alzu'bi, H.; Allateef, I.; Zweiri, Y.; Alkhateeb, B.; Al-Masarwah, I. Quad tilt rotor Vertical Take Off and Landing (VTOL) Unmanned Aerial Vehicle (UAV) with 45 degree rotors. Patent US20130105635, 2 May 2013.
26. Ryll, M.; Bühlhoff, H.H.; Giordano, P.R. First flight tests for a quadrotor UAV with tilting propellers. In Proceedings of the 2013 IEEE International Conference on Robotics and Automation, Karlsruhe, Germany, 6–10 May 2013; pp. 295–302. [[CrossRef](#)]
27. Ryll, M.; Bühlhoff, H.H.; Giordano, P.R. A Novel Overactuated Quadrotor Unmanned Aerial Vehicle: Modeling, Control, and Experimental Validation. *IEEE Trans. Control Syst. Technol.* **2015**, *23*, 540–556. [[CrossRef](#)]
28. Zortrax. Zortrax M200. 2016. Available online: <https://zortrax.com/printers/zortrax-m200/> (accessed on 28 September 2017).
29. Guzman, M. Modeling and Simulation of an Over-Actuated Dual Tilting Rotors Quadcopter. Master's Thesis, Kingston University, London, UK, 2015.
30. Lim, H.; Park, J.; Lee, D.; Kim, H.J. Build Your Own Quadrotor: Open-Source Projects on Unmanned Aerial Vehicles. *IEEE Robot. Autom. Mag.* **2012**, *19*, 33–45. [[CrossRef](#)]



© 2018 by the authors. Licensee MDPI, Basel, Switzerland. This article is an open access article distributed under the terms and conditions of the Creative Commons Attribution (CC BY) license (<http://creativecommons.org/licenses/by/4.0/>).